

Predicting Lane-by-Lane Flows and Speeds for Freeway Segments

Fabio Sasahara

University of Florida
518 Weil Hall - Gainesville, FL 32611
Phone: (352) 614-8886
Fax: (352) 392-3394
fsasahara@ufl.edu

Luan Guilherme Staichak Carvalho

University of Florida
518 Weil Hall - Gainesville, FL 32611
Phone: (352) 745-9423
Fax: (352) 392-3394
lstaichakcarvalh@ufl.edu

Tanay Datta Chowdhury

University of Florida
518 Weil Hall - Gainesville, FL 32611
Phone: (907) 346-0055
Fax: (352) 392-3394
tchowdhury1@ufl.edu

Zachary Jerome

University of Florida
511 Weil Hall - Gainesville, FL 32611
Phone: (865) 466-1638
Fax: (352) 392-3394
zjerome@ufl.edu

Lily Elefteriadou

University of Florida
512 Weil Hall - Gainesville, FL 32611
Phone: (352) 294-7802
Fax: (352) 392-3394
elefter@ce.ufl.edu

Alexander Skabardonis

University of California - Berkeley
109 McLaughlin Hall, Berkeley, CA 94720
Phone: (510) 642-9166
Fax: (510) 643-3955
skabardonis@ce.berkeley.edu

Word Count: 6097 words + 3 tables *(250) = **6847**
Submission date: **08/01/2019**

1 **ABSTRACT**

2 The main purpose of this research is to develop a series of models for estimating flows and
3 speeds by lane for various types of freeway segments. These models consider v/c , the presence of
4 trucks, grade, and the presence of upstream and downstream ramps. In order to predict lane
5 performance effectively, it is critical that capacity and free-flow speeds are also determined for
6 individual lanes. Therefore, this study also investigates the relationship between segment average
7 values and lane values for free-flow speeds and capacities, and proposes a method to estimate these
8 parameters for each lane as a function of the segment average. Speed and flow data were collected
9 from 48 segments throughout the US, including basic, merge and diverge segments, to develop
10 flow and speed distribution models.

11

12

13 *Keywords:* Highway Capacity, Freeways, Lane Distribution, Performance Measurement, Quality
14 of Service, Traffic Distribution, Traffic Flow, Speed

1. INTRODUCTION

The Highway Capacity Manual (HCM) [1] is used widely in evaluating traffic conditions both for operational and planning purposes.

One of the key limitations of the manual is the assumption that lanes perform equally, which does not correspond to field conditions and can result in inaccuracies in performance estimation. Understanding how individual lanes operate is critical for modeling congested conditions, especially at ramp junctions. The effects of ramps on the mainline traffic are not uniform, with congestion typically forming on the shoulder lanes, while median lanes may remain uncongested. Failure to model these conditions can lead to inaccurate performance estimations for such segments.

A more accurate model to predict individual lane performance can also be useful for planning purposes of traffic management strategies. By understanding how lanes perform differently, new strategies can be planned to encourage or discourage the use of certain lanes in a manner to optimize system performance.

With the development of travel time measures, new procedures to obtain origin-destination travel times would greatly benefit from methods that are able to predict individual lane performance, since the specific set of chosen lanes in a trip can impact total travel time. Therefore, new methods would be required to assess the performance of individual lanes on freeway facilities.

A literature review shows that a significant amount of research has been dedicated to increase understanding of traffic flow patterns on individual lanes, especially flow distribution. However, no research was found regarding the application of lane-by-lane performance in the HCM methods. With this motivation, Sasahara et al [2] investigated factors that affect lane flow distribution in basic freeway segments, including v/c , presence of heavy vehicles, and the ratio of ramp volume-to-distance. Additionally, the authors observed that weekends and nighttime can also affect flow distribution patterns differently. Speed predictions were performed in a lane-by-lane basis using individual inputs of capacity and free-flow speed, resulting in satisfactory results.

The authors advised, however, that good results were obtained because lane capacities and free-flow speeds were measured from field data. Practitioners, however, are unlikely to have measurements of free-flow speed and capacity on individual lanes to be used as inputs on HCM analyses. Additionally, the proposed methodology was focused on basic segments and did not consider other segments such as merge, diverge and weaving.

Based on the limitations from the previous work, the objective of this research is to develop and expand a series of models for estimating flows and speeds by lane for various types of freeway segments, including basic, merge and diverge segments. This study also investigates the relationship of segment averages to individual lane values for free-flow speeds and capacities. These models consider v/c , the presence of trucks, grade, and the presence and distances of upstream and downstream ramps.

2. LITERATURE REVIEW

Modeling of lane-by-lane flows and speeds requires determination of capacity and free-flow speed. The flow distribution by lane is affected by the demand-to-capacity ratio, and thus capacity must be known. Also, operating speed is a function of free flow speed, and estimating it requires the development of speed-flow models by lane. Therefore, both capacity and free flow

1 speed must be determined in order to produce lane-by-lane speed and flow models. This section
2 first provides an overview of the literature regarding capacity estimation, free-flow speed, both for
3 segments and for individual lanes. Next, it provides an overview of previously developed models
4 for lane-by-lane analysis, and it briefly discusses the impact of trucks and other factors on freeway
5 operations. The last paragraph summarizes the literature review findings.

6 Effectively measuring freeway performance requires accurate estimation of capacity.
7 Asgharzadeh and Kondyli [3] compared well-known capacity estimation methods, listing their
8 advantages and disadvantages: Van Aerde [4], Product Limit Method [5] [6], Sustainable Flow
9 Index [7] and HCM 6th Edition [1]. With the exception of Van Aerde, all methods rely on
10 breakdown identification, which brings the substantial advantage of addressing the stochastic
11 nature of capacity. Breakdown observation and its criteria have been discussed by several authors,
12 who suggest different threshold values for parameters such as speed drop and flow aggregation
13 period. ([6] [8] [9] [10]).

14 A growing body of literature supports the argument that HCM equations may be
15 overestimating capacity values for freeways. Elefteriadou et al [11] measured capacities in Florida
16 using the 85th percentile pre-breakdown flow approach. The researchers recommended, for urban
17 freeway merge/diverge segments, a capacity value of 2,100 pc/h/ln (3-lane) and 2,000 pc/h/ln (2
18 and 4+ lanes), which is significantly lower than the base capacity of 2,400 pc/h/ln recommended
19 by the HCM. Shojaat et al [7] proposed a new Sustainable Flow Index method, which yielded
20 capacities ranging from 1574 veh/h/ln to 2088 veh/h/ln for a 4-lane freeway segment in Frankfurt,
21 Germany. Rouphail et al [12] compared field-measured capacities to HCM-estimated values and
22 confirmed the findings from the previously mentioned capacity estimates.

23 Capacity and breakdown, on a lane-by-lane basis, has not been explored as extensively.
24 Xie et al [13] observed congested off-ramps in California to study heterogenous capacity
25 distribution among freeway lanes. The authors adopted a Bayesian model approach and indicated
26 that capacity differs among lanes within a freeway section, with higher values for leftmost lanes
27 and lower on rightmost lanes. Ma et al [14] proposed a method to identify breakdowns on
28 individual lanes, based on four diverge segments in Japan. The authors verified that shoulder lanes
29 typically experience breakdown at lower flow rates, and higher ramp demands contribute to
30 increase breakdown probability. Goto et al [15] analyzed the occurrence of breakdown in
31 individual lanes based on a freeway 2-lane merge segment in Japan. The authors found that
32 shoulder lanes consistently break down at a lower volume when compared to median lanes (300
33 veh/h difference between lanes), and indicate that smaller analysis intervals produce more accurate
34 results (1 minute was recommended).

35 Research on free-flow speeds on individual lanes has been limited. Van Zwet et al. [16]
36 indicate that free flow speeds vary among different lanes as a function of the number of lanes. The
37 authors proposed default values for free-flow speeds by lane depending on the number of lanes,
38 based on data from California detectors. Balakrishnan and Sivanandan [17] analyzed free-flow
39 speed variations in Indian roads and observed that free-flow speeds are higher on median lanes
40 compared to shoulder lanes.

41 A few studies in the literature have investigated flow distribution among freeway lanes.
42 Pompigna and Rupi [18] studied basic 3-lanes segments in Italy, and found that flow distribution
43 can be modeled as a function of demand-to-capacity ratio. For free flow conditions, flow is mostly
44 concentrated on the center lane for low demand conditions, but on congested scenarios the leftmost
45 lane carries the majority of the flow. Xiao et. al [19] studied the flow distribution on 2-lane
46 segments. The authors observed a high correlation of flow distribution and v/c ratio, with the

1 majority of flow concentrated in the rightmost lane for low demand conditions. As demand reaches
2 capacity, the flow concentration in the leftmost lane increases significantly. Lee and Park [20]
3 studied basic segments with 2, 3 and 4 lanes. For segment with 2 and 3 lanes, results are consistent
4 with the studies previously mentioned. For 4-lane segments, the authors found that center lanes
5 (lanes 2 and 3) have higher demand during low- flow conditions. When close to capacity, the
6 leftmost lane carries the majority of the flow.

7 Although a significant amount of research on lane flow distribution is available, research
8 on speed-flow models by lane is scarce. Previous research by Sasahara et al [2] explored speed-
9 flow models on individual lanes on basic segments only.

10 The presence of heavy vehicles is a key influencing factor in highway capacity, and
11 understanding how truck volumes distribute among freeway lanes under varying operational
12 conditions is critical for producing accurate lane-by-lane models. However, available literature is
13 scarce on this topic. Yousif et al [21] studied the distribution of heavy vehicles in UK motorways
14 and developed a few regression models using different predictors, such as HV flow, total flow and
15 speeds. However, the obtained models showed poor correlation values. Fwa and Li [22] have
16 analyzed lane distribution of truck traffic in Singapore roads, and found that the concentration of
17 heavy truck traffic in shoulder lanes increases as the segment total flow also increases. Caution
18 must be used, however, as truck traffic characteristics vary greatly among different locations as
19 function of diverse factors as speed limits, vehicle characteristics, truck lane restrictions, etc. No
20 study based on US roads was found in the literature review.

21 In summary, the following were concluded from the literature review:

- 22 • Previously developed models for lane-by-lane analysis have shown a strong
23 correlation of flow distribution and the segment v/c ratio, with different patterns
24 depending on the number of lanes. Additional factors such as ramp demand,
25 presence of heavy vehicles and even time of day and weekends can also affect the
26 flow distribution.
- 27 • Capacity and free-flow speed are not uniform among lanes, and the correct
28 estimation of these parameters on a lane-by-lane basis is critical to develop
29 individual speed-flow models.
- 30 • The capacity estimates provided by HCM methods may be overestimated when
31 compared to field data – this difference becomes more critical for lane-by-lane
32 analysis .
- 33 • Literature on truck distribution and speed distribution among freeway lanes is
34 extremely limited.

36 **3. DATABASE DESCRIPTION AND PRELIMINARY ANALYSIS**

37 The data collected for this study include speed and flow data from selected detector station sensors
38 in California, Virginia, Utah, Wisconsin, Minnesota, and Florida. These locations represent diverse
39 operational, design and behavioral conditions across the US, including the variability in driver lane
40 changing decisions. Sites were selected based on the following criteria:

- 41 • Speed and flow data were available for each lane, aggregated in 15-min intervals, for a
42 period of at least one year;

- Absence of freeway management strategies, such as express or high-occupancy vehicle (HOV) lanes, ramp metering, speed harmonization, or demand shoulder use;
- For merge and diverge and segments, good health detector data was available for the upstream, downstream and ramp sections;
- Percentages of heavy vehicles were available.

The final dataset included 48 locations: 19 basic, 14 merge, and 15 diverge segments with 2, 3 or 4 lanes on each direction. No 5-lane segments were included as many of the identified locations operate with HOV lanes. The number of required detector stations is different for each studied segment type. Basic segments require only one detector station. Diverge segments require two stations: one at the ramp influence area (upstream of the exit) and one along the ramp. Merge segments require three stations : one at the ramp influence area (downstream the merge), one along the ramp and one upstream of the merge.

Table 1 summarizes the dataset used for this study.

Table 1 - Data collection locations

Scenario	# of Sites	% Grade range ([min, max])	% HV Range ([min, max])	# Adjacent Ramps ([min, max])	States (# of Sites)	
Basic	2L	4	[-1.2, 0.5]	[1.0, 18.0]	[0, 2]	CA (1), MN (1), UT (1), VA (1)
	3L	8	[-3.1, 1.45]	[4.0, 32.9]	[0, 3]	CA (2), FL (1), MN (1), UT (2), VA (1), WI (1)
	4L	7	[-1.1, 1.7]	[4.4, 28.2]	[0, 1]	CA (3), FL (3), UT (1)
Merge	2L	4	[0.0, 2.7]	[11.8, 17.6]	[0, 1]	FL (2), UT (2)
	3L	8	[-0.9, 1.8]	[8.6, 27.9]	[0, 1]	CA (2), UT (5), MN(1)
	4L	2	[0.0, 2.71]	[1.3, 2.1]	[0, 1]	CA (2)
Diverge	2L	5	[-2.0, 0.8]	[3.4, 16]	[0, 1]	CA (2), FL (1), UT (1), WI (1)
	3L	8	[-2.2, 0.0]	[8.0, 19.7]	0	CA (3), UT (3), MN(2)
	4L	2	[0.7, 1.5]	[2.21, 5.1]	[1, 4]	CA (2)
TOTAL	48					

Speed and flow detector data were collected from online platforms of the respective state agencies ([23] [24] [25] [26] [27]). Downloaded data included volume and speed values for each lane aggregated at 15-min intervals, over a 1-year period for each location. Close observations were made on each detector’s health in order to avoid erroneous speed and flow data. Observations with erroneous or invalid data were excluded. Moreover, any observations showing events such as crashes, lane closures, and work zones were removed from the related detector data set. In this paper, lane 1 is also the rightmost.

Additional steps were necessary to ensure homogeneity on data aggregation along all sources. For our purposes, we aggregated the data on all locations to 15-min intervals and excluded holidays and weekends. These final treated datasets were used for capacity estimations and lane-by-lane speed estimation curves.

The heavy vehicle percentage (HV%) was collected from the respective state agencies. Average truck percentages are typically reported on an annual basis by agencies; therefore the

1 speed-flow data from detectors were downloaded only for periods when HV% information was
 2 available. The presence of ramps upstream or downstream of a site might cause significant impact
 3 on lane flow distribution. Therefore, the analysis included the number of such ramps within a half-
 4 mile upstream and downstream of the segment (access point density).
 5

6 4. LANE-BY-LANE FLOW MODELS BY SEGMENT TYPE

7 This section first discusses the estimation of capacity by segment type and then presents the models
 8 developed to estimate the percent of flow by lane as a function of selected parameters.

9 Capacity was estimated for each segment individually using the breakdown method, with
 10 a similar approach to the HCM guidance. Only data between 6:00 AM and 10:00 PM were used.
 11 The upstream detector is used for the capacity analysis of basic and diverge segments, while the
 12 downstream detector is used for merges. The segment FFS is estimated as average of all speed
 13 observations taken at flows no higher than 450 veh/h/ln, and breakdown is assumed to occur
 14 whenever a speed difference greater than 15% of the FFS is identified between two consecutive
 15 15 minutes observations. If two or more breakdowns are observed within one hour, only the first
 16 occurrence is registered. A capacity measurement is the flow observation at the time interval
 17 immediately before a breakdown. The estimated segment capacity is the 85th percentile of those
 18 capacity measurements.

19 Using these estimated segment capacities, we developed lane-by-lane flow estimation
 20 curves by analyzing each segment individually. The first step was to prepare each segment dataset.
 21 From the final treated datasets, only observations with flow less than capacity were used.
 22 Therefore, all demand-to-capacity (v/c) ratios range from 0 to 1.

23 The dataset was also cleaned to ensure it has a uniform distribution of v/c values across
 24 sites, in order to avoid biasing the regression model. For each site, observations are grouped in
 25 bins based on the v/c ratio, each with 0.1 range: (i.e: 0-0.1, 0.1-0.2, 0.2-0.3, ..., 0.9-1.0). Then, the
 26 bin with the smallest number of observations was set as a reference. For all other bins, observations
 27 were removed to match the number of observations of the smallest bin. This procedure ensures the
 28 dataset has a uniform distribution across v/c groups.

29 The *lane flow ratio* (LFR) model for each lane is estimated as a function of the logarithm
 30 of the segment v/c . This relationship was established empirically after evaluating the performance
 31 of logarithmic and polynomial regressions. Although a 4th degree polynomial provided an overall
 32 slightly better fit, the number of adjustment factors required to accommodate parameters of
 33 geometry (grade and number of accesses) and flow (truck percentile and ramp flow) was
 34 considered too high. Thus, a logarithmic model was selected as a balance between model
 35 complexity and accuracy. The flow estimation curves for each lane are fitted using the least squares
 36 method, except for the leftmost lane, which is estimated as the remaining flow, to ensure the sum
 37 of the flow shares from each lane always equals 100%. The equations estimating LFR are as
 38 follows:
 39

$$40 \quad LFR_i = \max(0, f_a \cdot \ln\left(\frac{v}{c}\right) + f_c) \quad \text{(Equation 1)}$$

$$42 \quad LFR_n = 1 - \sum_1^{n-1} LFR_i \quad \text{(Equation 2)}$$

44 Where:

1
2 LFR_i – share of the total flow on lane i , where i ranges from 1 to $n-1$ (n = total
3 number of segment lanes)

4 LFR_n – share of the total flow on the leftmost lane (lane n);

5 f_a – adjustment factor for a (Equation 3);

6 v/c – volume/capacity ratio ($0 < v/c \leq 1$), with volume measured on the
7 upstream detector;

8 f_c – adjustment factor for c (Equation 4);
9

10 The model proposed in Equation 1 can be applied for basic, merge and diverge segments.
11 For basic segments, obtaining v/c ratio is straight-forward as no changes are required to the current
12 methodology. For merge and diverge segments, the v/c ratio is estimated as follows:
13

- 14 • v : flow rate upstream the ramp (v_f) (veh/h)
- 15 • c : capacity of an equivalent basic segment with the same number of lanes (veh/h)

16
17 The adjustment factors f_a and f_c applicable in the analysis of basic segments are as follows:
18

$$19 \quad f_a = a + G \cdot f_{a,G} + t \cdot f_{a,t} + n \cdot f_{a,n} \quad \text{(Equation 3)}$$

$$20 \quad f_c = c + G \cdot f_{c,G} + t \cdot f_{c,t} + n \cdot f_{c,n} \quad \text{(Equation 4)}$$

21
22
23 For merge and diverge segments, the f_a and f_c factors are as follows, with additional
24 coefficients $f_{a,vR}$ and $f_{c,vR}$ to address ramp demand:
25

$$26 \quad f_a = a + G \cdot f_{a,G} + t \cdot f_{a,t} + n \cdot f_{a,n} + \frac{v_R}{1000} \cdot f_{a,vR} \quad \text{(Equation 5)}$$

$$27 \quad f_c = c + G \cdot f_{c,G} + t \cdot f_{c,t} + n \cdot f_{c,n} + \frac{v_R}{1000} \cdot f_{c,vR} \quad \text{(Equation 6)}$$

28
29
30 where:

31 G – grade (%);

32 a – empirical constant;

33 $f_{a,G}$ – adjustment factor due to impact of grade;

34 $f_{c,g}$ – adjustment factor due to impact of grade;

35 t – truck percentage (%);

36 $f_{a,t}$ – adjustment factor due to impact of trucks;

37 $f_{c,t}$ – adjustment factor due to impact of trucks;

38 n – access point density – number of ramps half a mile upstream and half mile
39 downstream;

40 $f_{a,n}$ – adjustment factor due to impact of access point density;

41 c – empirical constant;

42 $f_{c,n}$ – adjustment factor due to impact of access point density;

43 v_R – ramp flow (vph);

44 $f_{a,vR}$ – adjustment factor due to impact of ramp flow;
45

$f_{c,vR}$ – adjustment factor due to impact of ramp flow;

The empirical constants $a, c, f_{a,G}, f_{c,G}, f_{a,t}, f_{c,t}, f_{a,n}, f_{c,n}, f_{a,vR}, f_{c,vR}$, were obtained by regression and are specific for each combination of segment type, lane number and total number of lanes. The obtained values are presented in Table 2.

Table 2 – Adjustment factors for lane flow distribution

Lane #	Parameter	Basic segments			Diverge segments			Merge segments		
		2 lanes	3 lanes	4 lanes	2 lanes	3 lanes	4 lanes	2 lanes	3 lanes	4 lanes
L1	a	0.21012	-0.01041	0.06500	-0.15816	-0.11560	0.02250	-0.10486	0.00214	-0.14233
	c	0.60974	0.23707	0.21583	0.25377	0.19414	0.47982	0.41411	0.26199	0.41795
	f_{a,g}	0.02572	0.01096	-0.01298	0.02402	0.03721	0.00407	0.02344	-0.00429	0.00010
	f_{a,t}	-0.01828	-0.00265	-0.00194	0.00901	0.00255	-0.01221	-0.00168	-0.00271	-0.00037
	f_{a,n}	-0.14364	-0.00180	-0.07569	0.03052	-0.01365	0.00486	-0.01900	-0.00429	0.09622
	f_{c,g}	-0.01199	0.00052	-0.03795	0.01669	0.00619	-0.02882	0.02841	0.03578	0.06412
	f_{c,t}	-0.01054	-0.00190	0.00263	0.01955	0.00289	-0.05490	-0.00316	-0.00127	-0.10810
	f_{c,n}	-0.06612	0.03680	-0.03306	0.10574	0.03588	-0.02254	-0.05626	-0.02959	-0.11612
	f_{a,vR}				-0.06526	-0.07129	-0.00046	0.00885	-0.08349	0.02680
	f_{c,vR}				0.03249	0.05277	-0.01673	-0.00012	-0.02960	0.00791
L2	a		-0.05337	-0.02225		0.01587	-0.02909		0.00502	-0.04081
	c		0.32879	0.28060		0.34506	0.48531		0.37648	0.43279
	f_{a,g}		-0.00248	0.00114		-0.03173	0.00172		-0.01004	0.00331
	f_{a,t}		0.00088	0.00029		-0.00152	-0.00295		-0.00183	0.00229
	f_{a,n}		0.00078	-0.01142		0.01614	0.00759		0.00227	-0.00834
	f_{c,g}		-0.01246	-0.02161		-0.02412	-0.02351		0.01496	0.00164
	f_{c,t}		0.00209	-0.00002		-0.00004	-0.04124		-0.00049	-0.07804
	f_{c,n}		0.00819	-0.03565		0.03220	-0.02455		-0.00954	-0.09533
	f_{a,vR}					-0.03433	-0.00743		-0.12506	-0.03528
	f_{c,vR}					-0.06997	-0.00970		-0.05233	-0.01213
L3	a			-0.04458			-0.02612			0.01518
	c			0.28550			0.48683			0.43882
	f_{a,g}			-0.00048			-0.00013			-0.00284
	f_{a,t}			0.00215			0.00164			-0.00108
	f_{a,n}			0.01611			0.00015			-0.00041
	f_{c,g}			0.00685			-0.02512			0.01977
	f_{c,t}			-0.00138			-0.02769			-0.05081
	f_{c,n}			0.02664			-0.02585			-0.08293
	f_{a,vR}						0.02389			-0.07713
	f_{c,vR}						-0.00693			-0.04123

A practical application of the LFR model is presented next for a 3-lane diverge segment (single period analysis), with the following input data:

- Grade (G): 3%
- Heavy vehicles (t): 4%
- Access point density (n): 2 adjacent ramps
- Mainline demand flow rate (v): 5500 veh/h
- Off-ramp demand (v_R): 850 veh/h
- Measured segment capacity (c): 2050 veh/h/ln (6150 veh/h)

The flow ratio for lane 1 (right lane) is obtained by the following equation:

$$LFR_1 = \max\left(0, f_{a1} \cdot \ln\left(\frac{v}{c}\right) + f_{c1}\right)$$

The adjustment factors f_a and f_c for lane 1 are obtained as follows:

$$f_{a1} = a + G \cdot f_{a,G} + t \cdot f_{a,t} + n \cdot f_{a,n} + \frac{v_R}{1000} \cdot f_{a,vR}$$

$$f_{a1} = -0.11560 + 3 \cdot 0.03721 + 4 \cdot 0.00255 + 2 \cdot (-0.01365) + \frac{850}{1000} \cdot (-0.07129)$$

$$f_{a1} = -0.08166$$

$$f_{c1} = c + G \cdot f_{c,G} + t \cdot f_{c,t} + n \cdot f_{c,n} + \frac{v_R}{1000} \cdot f_{c,vR}$$

$$f_{c1} = 0.19414 + 3 \cdot 0.00619 + 4 \cdot 0.00289 + 2 \cdot 0.03588 + \frac{850}{1000} \cdot (0.05277)$$

$$f_{c1} = 0.3411$$

The flow rate on lane 1 can then be obtained by:

$$LFR_1 = \max\left(0, -0.08166 \cdot \ln\left(\frac{5500}{3 \cdot 2050}\right) + 0.3411\right)$$

$$LFR_1 = \mathbf{35.1\%}$$

The same procedure is applied to obtain the flow rate on lane 2, using the respective coefficients from Table 3:

$$f_{a2} = a + G \cdot f_{a,G} + t \cdot f_{a,t} + n \cdot f_{a,n} + \frac{v_R}{1000} \cdot f_{a,vR}$$

$$f_{a2} = 0.01587 + 3 \cdot (-0.03173) + 4 \cdot (-0.00152) + 2 \cdot 0.01614 + \frac{850}{1000} \cdot (-0.03433)$$

$$f_{a2} = -0.0823$$

$$f_{c2} = c + G \cdot f_{c,G} + t \cdot f_{c,t} + n \cdot f_{c,n} + \frac{v_R}{1000} \cdot f_{c,vR}$$

$$f_{c2} = 0.34506 + 3 \cdot (-0.02412) + 4 \cdot (-0.00004) + 2 \cdot 0.0322 + \frac{850}{1000} \cdot (-0.06997)$$

$$f_{c2} = 0.27746$$

$$LFR_2 = \max\left(0, -0.0823 \cdot \ln\left(\frac{5500}{3 \cdot 2050}\right) + 0.27746\right)$$

$$LFR_2 = \mathbf{28.7\%}$$

Finally, the flow rate on the leftmost lane (lane 3) can be obtained as follows:

1 $LFR_3 = 1 - LFR_2 - LFR_1 = 1 - 0.287 - 0.351$
2 $LFR_3 = 36.2\%$
3

4 **5. SPEED FLOW CURVES BY LANE AND BY SEGMENT TYPE**

5 This section presents the models developed to obtain speed-flow curves for each lane in a freeway
6 segment, as a function of two key inputs: free-flow speed (FFS) and lane capacity. The first part
7 of the section discusses the estimation of lane FFS, while the next part presents models for
8 obtaining lane capacities. The last part provides the speed-flow models obtained as a function of
9 lane FFS and lane capacities.

10
11 **Lane FFS**

12
13 Field observations have shown ([16] [17]) that operating speeds differ among lanes, and they are
14 typically lower in shoulder lanes and higher in median lanes. Based on the dataset previously
15 described in Table 1, FFS were measured as the average speed for segment flow rates below 450
16 veh/h/ln. This criterion is consistent with HCM guidance, which recommends measuring FFS for
17 flows no greater than 500 pc/h/ln.

18 Next, lane FFS were modeled as a function of the segment FFS and as a function of the
19 number of lanes on the segment, as shown in Figure 1. Due to the ramp influence on traffic flow,
20 merge and diverge segments are likely to have different distributions of FFS. Therefore, distinct
21 models were developed by segment type. Linear regression models were developed with the
22 intercept set to zero.

23 As it can be observed in Figure 1, there is a good correlation between segment and lane
24 FFS, confirming field observations: shoulder lanes' FFS are lower than the segment average, while
25 median lanes' FFS are higher. Center lanes typically have FFS values very close to the segment
26 average.
27

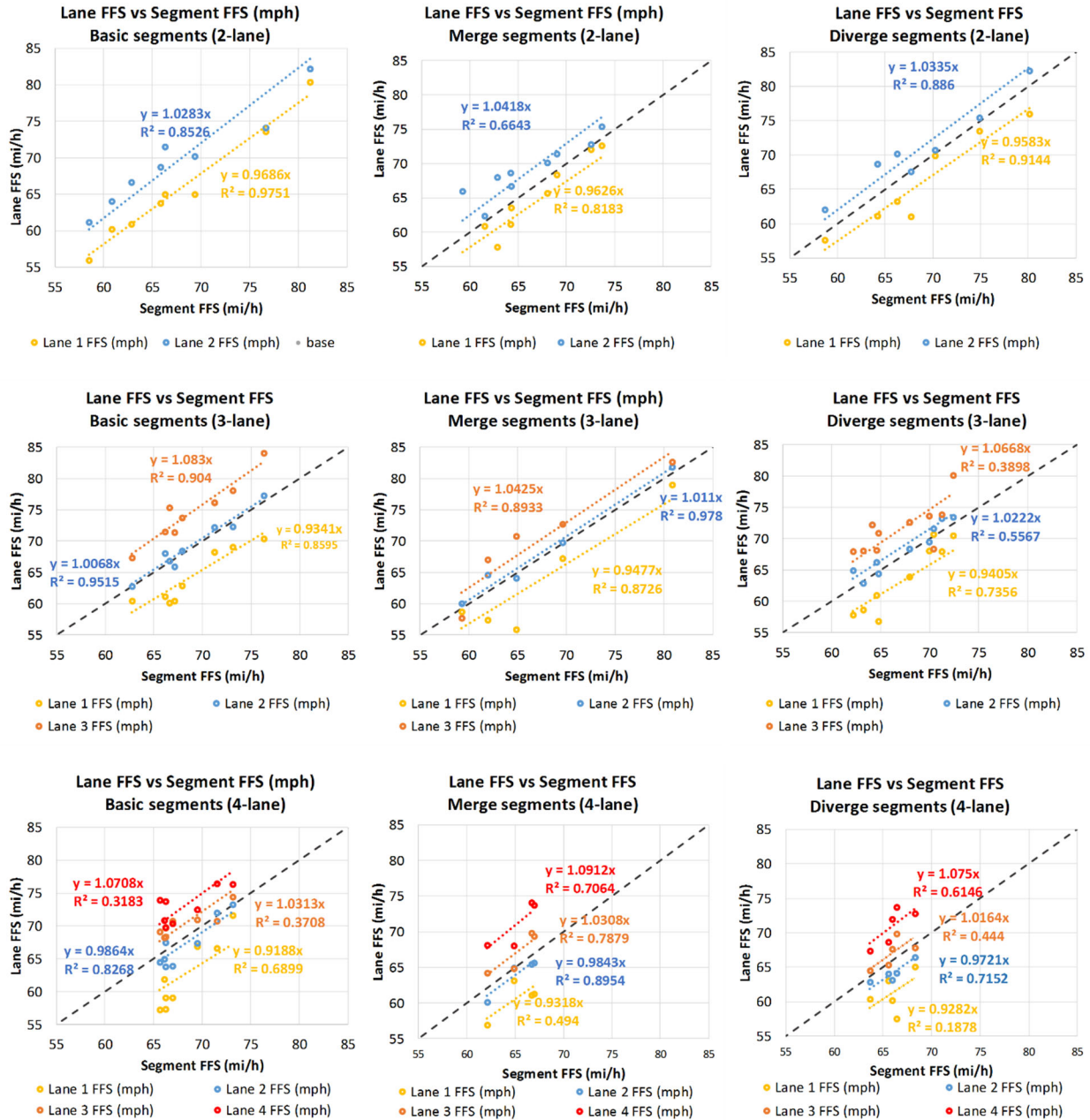


Figure 1 - Segment FFS and lane FFS, by segment type and number of lanes

Based on the obtained results, models were developed to estimate individual lane FFS by applying a multiplying factor to the segment FFS. These models are shown in Figure 1 for each lane. Table 3 summarizes the recommended multipliers which are provided as a function of the segment type and the number of lanes in the segment. As shown, when the number of lanes increases, the range of FFS multipliers increase as well (i.e. there are lower speeds in the shoulder lanes and higher speeds on the median lanes). For 2-lane segments, merge and diverge segments have a higher difference in FFS between the two lanes when compared to basic segments. For 3-lane segments, basic segments show the highest FFS range, while merge segments have more uniform lane FFS. As for 4-lane segments, merge segments show the highest FFS range, followed by basic and merge segments yield similar results.

1
2
3

Table 3 – Multipliers to estimate lane FFS from segment FFS

Segment type	Number of lanes	FFS Multiplier				Multiplier range
		L1	L2	L3	L4	
Basic	2 lanes	0.965	1.032			0.067
	3 lanes	0.934	1.010	1.087		0.153
	4 lanes	0.924	0.989	1.028	1.079	0.155
Merge	2 lanes	0.964	1.044			0.080
	3 lanes	0.955	1.015	1.045		0.090
	4 lanes	0.935	0.991	1.036	1.091	0.156
Diverge	2 lanes	0.961	1.035			0.074
	3 lanes	0.943	1.024	1.068		0.125
	4 lanes	0.933	0.975	1.018	1.074	0.141

4
5

Lane Capacities

7

8 Individual lane capacities were obtained through the breakdown observation approach, as
 9 described under Section 4. Although the literature shows that lanes may break down at different
 10 times, especially on ramp segments, using 15-min aggregated data allows using the assumption
 11 that all lanes break down within one time period.

12 The process for measuring lane capacities is illustrated in Figure 2 based on an example
 13 merge segment with 3 lanes. At the 85th percentile, the estimated segment capacity is 1561
 14 veh/h/ln. However, the 85th percentile approach for different lanes yields significantly different
 15 flows at breakdown (Figure 2a): 1132 veh/h/ln (lane 1), 1604 veh/h/ln (lane 2) and 2064 veh/h/ln
 16 (lane 3). These values are taken as the estimated capacities of individual lanes. When considered
 17 as the relative proportion of total flow, lane capacities can be estimated as 24%, 33% and 43% of
 18 total capacity for lanes 1, 2 and 3, respectively. Figure 2b shows the distribution of LFRs as a
 19 function of segment capacity. As observed, at higher volumes the flow distribution is stable at the
 20 time of breakdown, showing that lane capacities can be consistently measured using this approach.

21

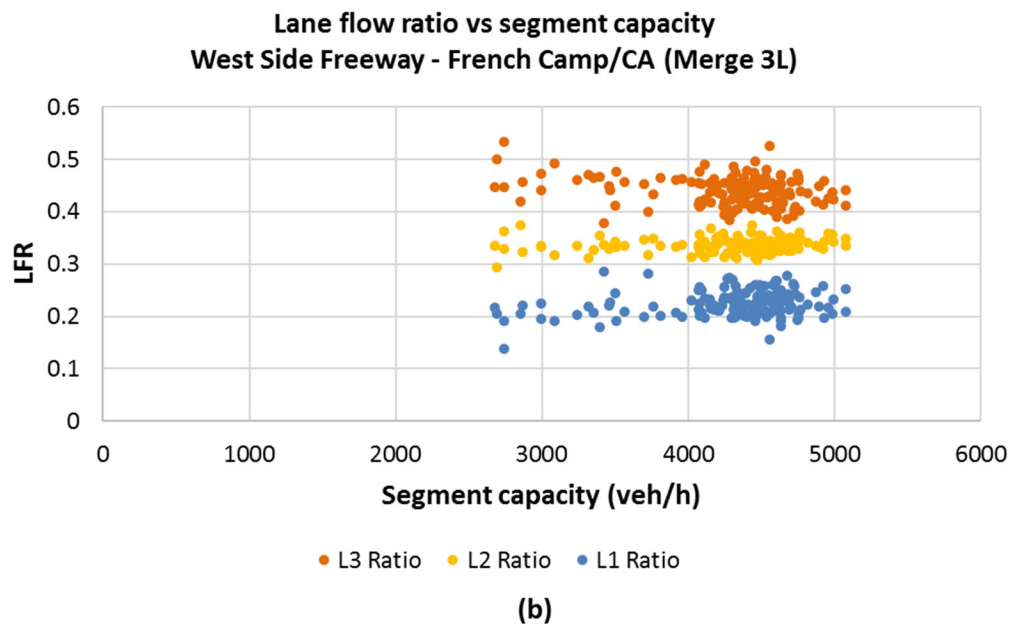
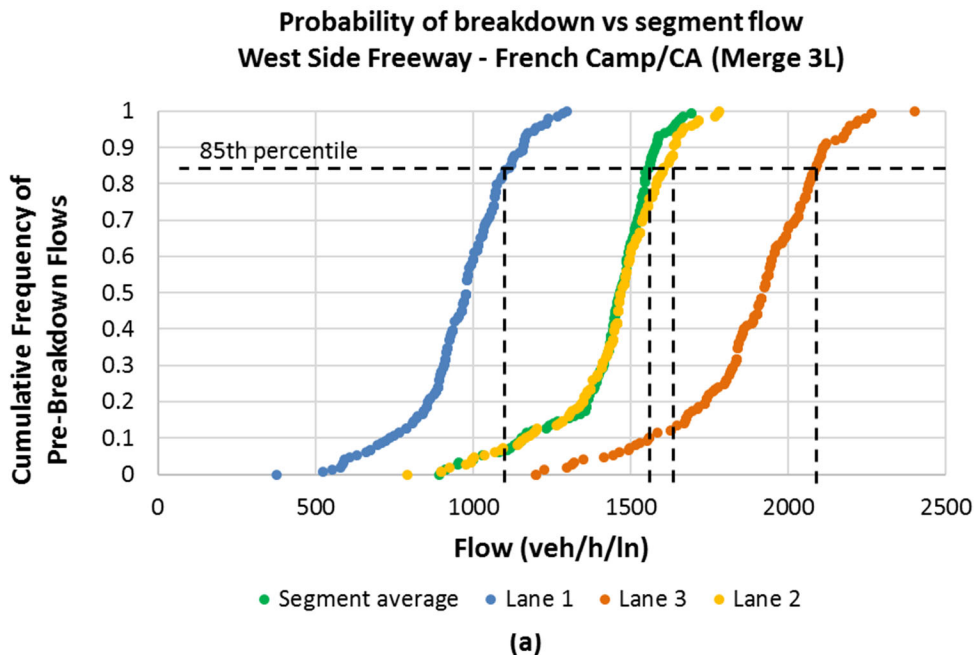
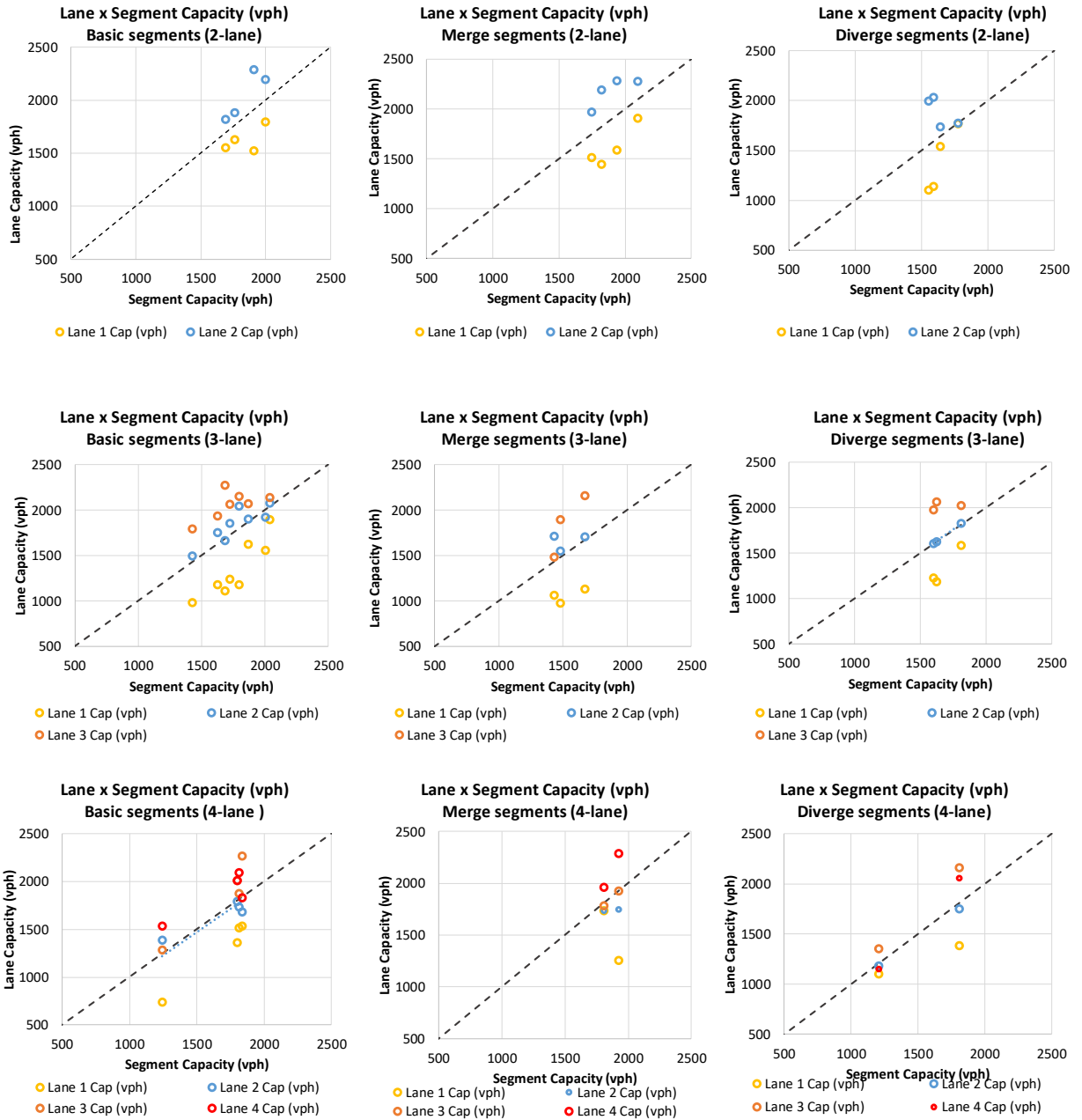


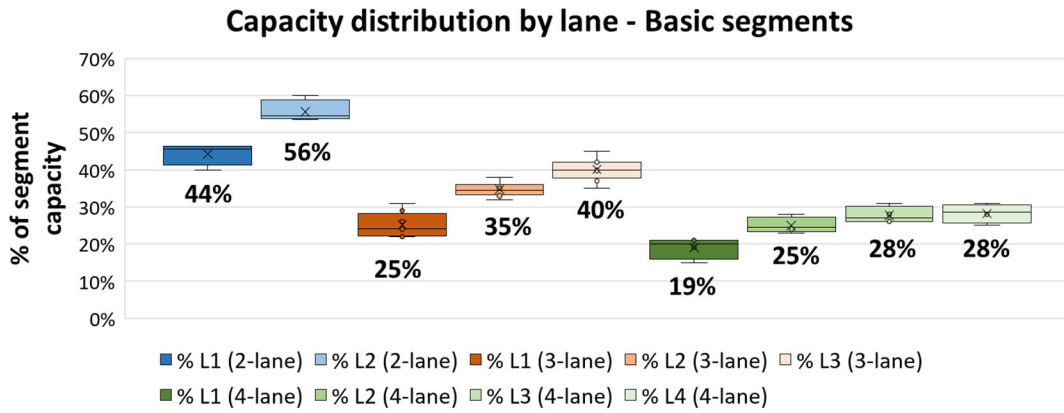
Figure 2 – Example of lane capacity estimation (French Camp/CA): (a) lane flow distribution at breakdown and (b) LFRs as a function of segment capacity

The same rationale was applied to all locations in the database. Figure 3 shows the relationship between the measured segment capacities and their respective capacities for individual lanes. As it can be observed, capacity typically increases from the rightmost to the leftmost lanes, with center lanes showing capacity values similar to the segment average.

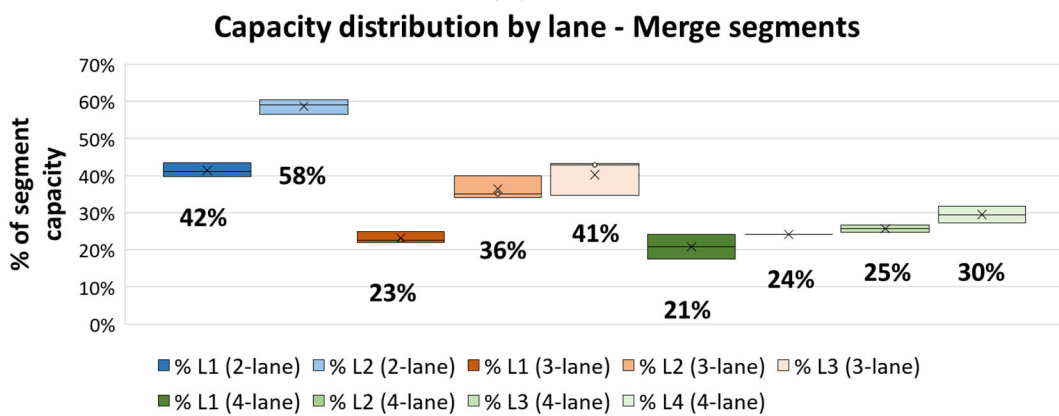


1
2
3 **Figure 3 – Relationship between segment capacity and individual lane capacity, by segment**
4 **type and number of lanes**

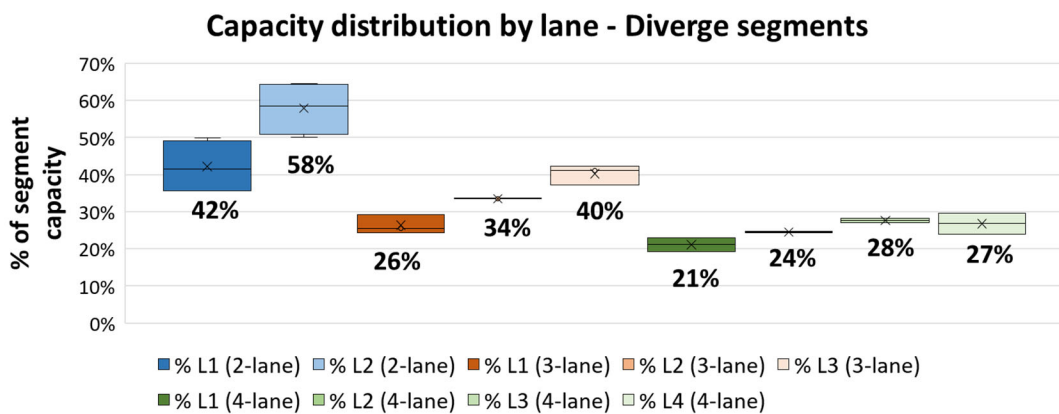
5
6 Next, results were averaged by segment type and number of lanes. Figure 4 presents the
7 percent distribution of the total segment capacity across lanes (the numbers below the whisker
8 boxes represent the average values of lane capacity).
9



(a)



(b)



(c)

Figure 4 – Capacity of individual lanes as a percentage of segment capacity, by segment type and number of lanes

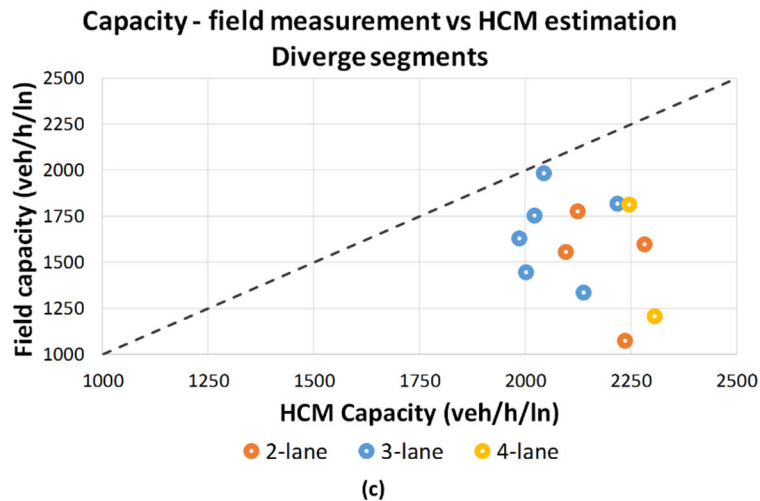
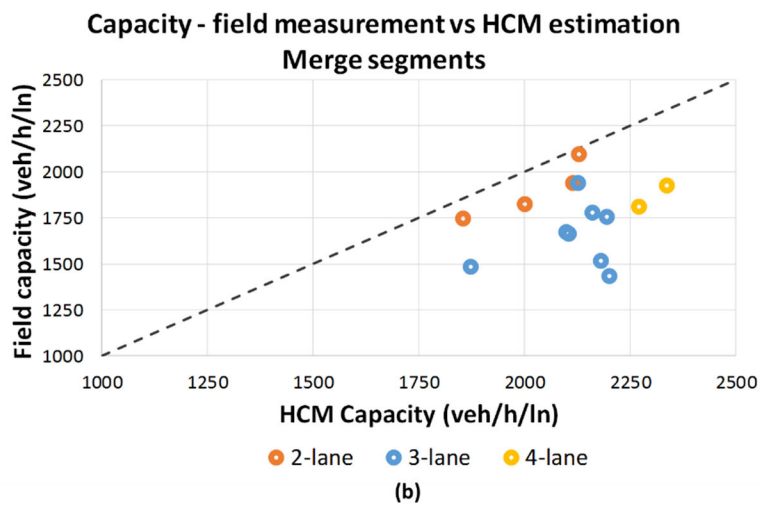
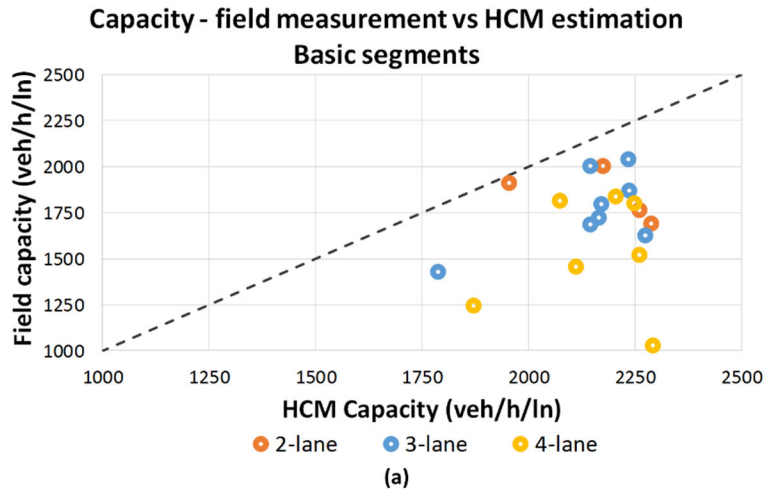
1
2
3
4
5

1 The segment capacities measured from field data may not be equal to the estimated
2 capacities using HCM methodologies. According to the HCM Equation 12-6, base capacity can be
3 estimated as:

$$c = \min[2200 + 10 x (FFS - 50), 2400] \quad \text{(Equation 7)}$$

4
5
6
7 For each location from the dataset, base capacity was calculated using Equation 7, as FFS
8 is available from field measurements. Since this equation provides capacity values in passenger-
9 car equivalents, a heavy vehicle factor f_{HV} (as defined in HCM Equation 12-10) was applied to
10 convert the base capacity to veh/h and then make the unit consistent with field data.

11 Figure 5 shows the comparison of capacity values measured from the field against
12 theoretical estimates using the HCM methods. All observations yielded field measurements
13 smaller than the estimated capacities provided by the HCM. When different segment types are
14 compared, however, no clear conclusions can be drawn on which lanes have higher differences
15 between field and estimated capacities. The field measurements of capacity are, on average, 21.7%
16 smaller than their respective HCM estimations. It is a significant difference that can lead to
17 inaccurate capacity analyses, as the HCM methodologies may overestimate capacity and therefore
18 overestimate the overall segment performance. For this reason, it is recommended that capacity
19 adjustment factors (CAFs) are applied to adjust the estimated capacities to local conditions.
20 Additional research is recommended to further investigate the calibration of CAFs.
21



1
2 **Figure 5 – Field measured and HCM estimated capacity values, for (a) basic segments, (b)**
3 **merge segments and (c) diverge segments**
4

1 With flow, capacity and FFS by lane determined, HCM equations can be used to estimate
 2 operating speeds on individual lanes. Segment-wise inputs of flow, capacity and FFS are based on
 3 the field measurements, and the developed methods previously described are applied to estimate
 4 their distribution among individual lanes.

5 For basic segments, average speed is determined as:

$$7 \quad S = FFS - \frac{(FFS - \frac{c}{45})(v_p - BP)^2}{(c - BP)^2} \quad \text{(Equation 8)}$$

8
 9 This model is applied to individual lanes, as the three key parameters (FFS, c and v_p) are
 10 input by lane. The breakpoint value (BP) is also determined for each lane (Equation 9).

$$11 \quad BP = [1000 + 40 \times (75 - FFS_{adj})] \times CAF^2 \quad \text{(Equation 9)}$$

12
 13 It is worth noting that a capacity adjustment factor (CAF) is considered in the estimation
 14 of the breakpoint. The HCM method defines the *adjusted capacity* c_{adj} as the product of the base
 15 capacity by a *capacity adjustment factor* (CAF), which typically reflects impacts of weather,
 16 incident, work zone, driver population, and calibration adjustments.

$$17 \quad c_{adj} = c \times CAF \quad \text{(Equation 10)}$$

18
 19 As field values of segment capacities were obtained, these can be inserted into Equation 7
 20 as the value of adjusted capacity. Therefore, CAFs become the single unknown in the equation and
 21 can be easily obtained.

22 A practical example was developed to verify and illustrate the developed methodology. A
 23 2-lane basic segment was modeled and the lane-by-lane performance is compared to field data
 24 (CA-1 NB – Santa Cruz/CA). Field measured parameters are as follows:

- 25 • Free-flow speed: 69.1 mph
- 26 • Capacity: 3993 veh/h (1996.5 veh/h/ln)
- 27 • % heavy vehicles: 1.7
- 28 • Grade: 3% (rolling)

29 By applying the multiplying factors obtained in Table 3 to the segment FFS, individual
 30 FFS can be obtained as follows:

- 31 • $FFS_1 = FFS \times 0.965 = 69.1 \times 0.965 = \mathbf{66.68 \text{ mph}}$
- 32 • $FFS_2 = FFS \times 1.032 = 69.1 \times 1.032 = \mathbf{71.31 \text{ mph}}$

33
 34 Next, lane capacities are obtained by applying the multiplying factors obtained in Figure
 35 4 to the capacity as follows:

- 36 • $c_1 = c \times 44\% = 3993 \times 44\% = \mathbf{1757 \text{ veh/h}}$
- 37 • $c_2 = c \times 56\% = 3993 \times 56\% = \mathbf{2236 \text{ veh/h}}$

1 For comparison purposes, HCM methods would obtain the following theoretical capacity
2 value:

3
4 • $c = [2200 + 10 \times (\text{FFS} - 50)] \times f_{\text{HV}} = [2200 + 10 \times (69.1 - 50)] \times 0.967$
5 $= \mathbf{2312 \text{ veh/h/ln}}$
6

7 Therefore, the recommended CAF for this location is obtained by dividing field measured
8 by theoretical values of capacity:

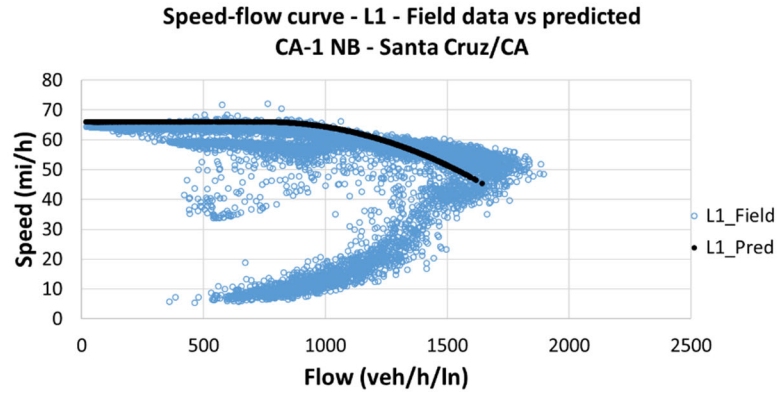
9
10 • $\text{CAF} = c_{\text{adj}}/c = 1996.5/2312 = \mathbf{0.864}$
11

12 Next, the breakpoint values for each lane can be obtained:

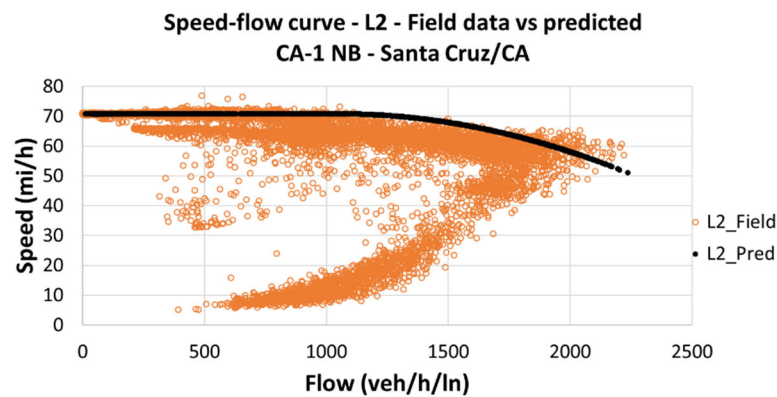
13
14 • $\text{BP}_1 = [1000 + 40 \times (75 - \text{FFS}_1)] \times \text{CAF}^2 = [1000 + 40 \times (75 - 66.68)] \times 0.864^2 =$
15 $= 995 \text{ veh/h}$
16

17 • $\text{BP}_2 = [1000 + 40 \times (75 - \text{FFS}_2)] \times \text{CAF}^2 = [1000 + 40 \times (75 - 71.31)] \times 0.864^2 =$
18 $= 857 \text{ veh/h}$
19

20 Flows on each lane can be obtained by applying the model described in Equation 1 to the
21 flow rate entering the segment. Next, speeds on individual lanes using the speed-flow relationship
22 described in Equation 8. For this location, a sample of 14690 observations (15-min each) was
23 randomly selected, and then predicted values are compared to field data in Figure 6.
24
25



(a)



(b)

Figure 6 – Field x predicted speed-flow curve for (a) Lane 1 and (b) Lane 2 (CA-1 NB – Santa Cruz/CA)

As observed, the individual speed-flow models can replicate field conditions with good accuracy. Naturally, the oversaturated portion of the curve cannot be addressed by the model, as this is already a limitation of the existing method.

6. CONCLUSIONS AND RECOMMENDATIONS

The methodology presented in this study expands previous work on lane-by-lane analysis on freeway segments, addressing gaps as ramp segments, percentage of heavy vehicles, grade, adjacent ramps, among others. Field measurements of free-flow speed and capacity were obtained for the studied locations for both segment-wise and individual lanes. Based on the obtained results, the following conclusions can be drawn:

- Free-flow speeds for individual lanes are highly correlated to the segment average, being lower on shoulder lanes and higher on median lanes. Therefore, a multiplier factor can be used to estimate lane free-flow speeds based on the segment average.

1
2
3
4
5
6
7
8
9
10
11
12
13
14
15
16
17
18
19
20
21
22
23
24
25
26

- No significant conclusions were found on whether free-flow speeds distribution among lanes is different depending on the segment type and number of lanes. Additional research is recommended to further investigate factors such as ramp geometry and demand as influencing factors on free-flow speeds.
- Similar to free-flow speeds, lane capacities also correlate to the segment average being lower on shoulder lanes and higher on median lanes. Nevertheless, the capacity of individual lanes can be modeled as a percent of the total segment capacity, being lower on shoulder lanes and higher on median lanes.
- Observed field capacities are significantly lower than the theoretical estimates obtained from HCM method (approximately 21%), which can lead to inaccurate performance estimation.

The following recommendations for future research are presented as follows:

- Expand the model to wider freeway segments, such as 5+ lanes.
- Expand the model to include weaving segments.
- Comparison of field-measured and HCM-estimated values for segment capacity, with further investigation of which factors are relevant to this difference and how CAFs can be calibrated to address this issue.

1 **ACKNOWLEDGMENTS**

2 This work was performed by the University of Florida Transportation Institute, and complements
3 the scope of the NCHRP Project Number 15-57: Highway Capacity Manual Methodologies for
4 Corridors Involving Freeways and Surface Streets. The authors acknowledge the valuable
5 contributions of members from the NCHRP 15-57 Panel and from the Highway Capacity and
6 Quality of Service Committee, who greatly facilitated the data collection process for this study.

7 The opinions and conclusions expressed or implied in this paper are those of the authors,
8 and not necessarily those of the TRB, the National Research Council, FHWA, AASHTO, or the
9 individual states participating in the NCHRP.

1 **AUTHOR CONTRIBUTION STATEMENT**

2
3 The authors confirm contribution to the paper as follows:

- 4
- 5 • **Study conception and design:** Fabio Sasahara, Luan Carvalho, Lily Elefteriadou,
6 Alexander Skabardonis
 - 7 • **Literature review:** Fabio Sasahara
 - 8 • **Methodology:** Fabio Sasahara, Luan Carvalho
 - 9 • **Data collection:** Tanay Chowdhury, Zachary Jerome, Fabio Sasahara
 - 10 • **Analysis and interpretation of results:** Fabio Sasahara, Luan Carvalho, Lily
11 Elefteriadou, Alexander Skabardonis
 - 12 • **Manuscript preparation:** Fabio Sasahara, Luan Carvalho, Lily Elefteriadou
- 13

14 All authors reviewed the results and approved the final version of the manuscript.

15

1 REFERENCES

2

- [1] Transportation Research Board, Highway Capacity Manual 6th Edition, Washington D.C, 2016.
- [2] F. Sasahara, L. Elefteriadou and S. Dong, "Lane-by-Lane Analysis Framework for Conducting Highway Capacity Analyses at Freeway Segments," *Transportation Research Record*, 2019.
- [3] M. Asgharzadeh and A. Kondyli, "Comparison of Highway Capacity Estimation Methods," *Transportation Research Record*, vol. 2672, no. 15, p. 75–84, 2018.
- [4] M. Van Aerde, "Single Regime Speed-Flow-Density Relationship for Congested and Uncongested Highways,," in *Annual Meeting of the Transportation Research Board*, Washington, DC, 1995.
- [5] W. Brilon, J. Geistefeldt and M. Regler, "Reliability of Freeway Traffic Flow: A Stochastic Concept of Capacity".
- [6] W. Brilon and H. Zurlinden, "Breakdown Probability and Traffic Efficiency as Design Criteria for Freeways," *Forschung Strassenbau und Strassenverkehrstechnik*, vol. 870, 2003.
- [7] S. Shojaat, J. Geistefeldt, S. Parr, C. Wilmot and B. Wolshon, "Sustained Flow Index: Stochastic Measure of Freeway Performance," *Transportation Research Record*, no. 2554, pp. 156-165, 2016.
- [8] A. Kondyli, B. St. George, L. Elefteriadou and G. Bonyani, "Defining, measuring and modelig capacity for the Highway Capacity Manual," *Journal of Transportation Engineering, Part A: Systems*, vol. 143, no. 3, 2017.
- [9] R. Kuhne and A. Ludtke, "Traffic breakdowns and freeway capacity as extreme value statistics," *Transportation Research Part C: Emerging Technologies*, vol. 27, pp. 159-168, 2013.
- [10] M. Lorenz and L. Elefteriadou, "A Probabilistic Approach to Defining Freeway Capacity and Breakdown," *Transportation Research Board Circular E-C018*, 2000.
- [11] L. Elefteriadou, A. Kondyli and B. S. George, "Estimation of Capacities on Florida Freeways (FDOT Report)," Gainesville, FL, 2013.
- [12] N. Rouphail, K. Pyo, T. Chase and M. Cetin, "Guidance for Field and Sensor-Based Measurement of HCM and Simulation Performance," College Park, 2018.
- [13] K. Xie, K. Ozbay and H. Yang, "The Heterogeneity Of Capacity Distributions Among Different Freeway Lanes," in *Celebrating 50 Years of Traffic Flow Theory*, Portland, 2015.
- [14] D. Ma, H. Nakamura and M. Asano, "Lane-Based Breakdown Identification at Diverge Sections for Breakdown Probability Modeling," *Transportation Research Record*, no. 2395, pp. 83-92, 2013.
- [15] A. Goto, D. Kato and H. Nakamura, "A Lane-based Analysis of Stochastic Breakdown Phenomena on an Urban Expressway Section," *Asian Transport Studies* , vol. 5, no. 1, pp. 64-80, 2018.

- [16] E. v. Zweet, C. Chen, Z. Jia and J. Know, "A statistical method for estimating speed from single-loop detectors," 2003. [Online]. Available: http://pems.dot.ca.gov/Papers/vanzwet_gfactor.pdf.
- [17] S. Balakrishnan and R. Sivanandan, "Influence of Lane and Vehicle Subclass on Free-flow Speeds for Urban Roads in Heterogeneous Traffic," in *18th Euro Working Group on Transportation*, Delft, The Netherlands, 2015.
- [18] A. Pompigna and F. Rupi, "Lane-Distribution Models and Related Effects on The Capacity for a Three-Lane Freeway Section: Case Study in Italy," *Journal of Transportation Engineering, Part A: Systems*, 2017.
- [19] C. Xiao, C. Shao, M. Meng, P. Wang and B. Wang, "Lane Flow Distribution of a Long Continuous Highway," *European Transport*, 2014.
- [20] J. Lee and B. Park, "Determining Lane Use Distributions Using Basic Freeway Segment Density Measures," *ASCE Journal of Transportation Engineering*, vol. 138, pp. 210-217, 2012.
- [21] S. Yousif, J. Al-Obaedi and R. Henson, "Drivers' Lane Utilization for United Kingdom Motorways," *Journal of Transportation Engineering - ASCE*, vol. 139, no. 5, pp. 441-447, 2013.
- [22] T. Fwa and S. Li, "Estimation of Lane Distribution of Truck Traffic for Pavement Design," *Journal of Transportation Engineering - ASCE*, vol. 121, no. 3, pp. 241-248, 1995.
- [23] "RITIS.org," University of Maryland, [Online]. Available: <https://ritis.org>. [Accessed July 2017].
- [24] "Caltrans PeMS," [Online]. Available: <http://pems.dot.ca.gov/>. [Accessed June 2019].
- [25] "MN Data Tools," [Online]. Available: <http://data.dot.state.mn.us/datatools/>. [Accessed June 2019].
- [26] "Utah DOT PeMS," [Online]. Available: <https://udot.iteris-pems.com/>. [Accessed June 2019].
- [27] "Virginia DOT PeMS," [Online]. Available: <https://vdot.iteris-pems.com/>. [Accessed June 2019].

1
2